Acta Scientiae Veterinariae, 2026. 54: 2010.

RESEARCH ARTICLE
Pub. 2010

ISSN 1679-9216

Computed Tomography of the Appendicular Skeleton and Arboreal Adaptations of *Bradypus variegatus*

Michel Santos e Cunha[1], Daniel Furtado Perdigão[2], José Gonçalo Monteiro Campos[2], Thiago da Silva Cardoso[1], Lucas Santos Carvalho[1], Luisa Pucci Bueno Borges[1], Sheyla Farhayldes Souza Domingues[1], Érika Renata Branco[3], Francisco Décio de Oliveira Monteiro[4] & Pedro Paulo Maia Teixeira[1]

ABSTRACT

***Background*:** The brown-throated sloth (*Bradypus variegatus*) is a highly specialized arboreal xenarthran whose unique suspensory locomotion in the Amazon canopy necessitates distinct morphological adaptations of its appendicular skeleton. While crucial for understanding its evolutionary niche, a comprehensive anatomical description of this skeletal system using modern computed tomography is lacking. This study aimed to provide a detailed computed tomography-based analysis of the *B. variegatus* appendicular skeleton, explicitly correlating the observed osteological features with functional demands of arboreal suspension and locomotion.

***Materials, Methods & Results*:** This descriptive anatomical study utilized 9 frozen cadavers of *B. variegatus* (6 young males, 3 young females). Specimens underwent helical computed tomography scanning in dorsal recumbency with limbs extended. Anatomical analysis was performed using multiplanar reconstructions and 3-dimensional volume rendering. Results detailed significant adaptations. The thoracic limbs were markedly larger than the pelvic limbs. The scapula presented a convex dorsal margin and a well-defined spina scapula; the clavicle was absent. The humerus was a long cylindrical bone (mean length: 9.17 cm). The radius and ulna were completely separated by a distinct interosseous space. The carpus consisted of 5 diffusely arranged bones, with metacarpals and phalanges adapted to support elongated claws. In the pelvic limb, the femur had a slightly curved diaphysis (mean mediolateral diameter: 7.51 mm); a patella was not observed. The tibia and fibula also featured an interosseous space. The pelvis was characterized by a deep, rounded acetabulum, a thin ischial tuberosity, a pubis with notable lateral amplitude, and a sacrum articulating with the ilium via 6 vertebrae. These features, including the disproportionate limb size, absent clavicle, fused carpal elements, and specialized pelvic architecture, are interpreted as direct adaptations for suspensory posture and arboreal mobility.

***Discussion*:** The morphological suite described, comprising disproportionately large thoracic limbs, a vestigial or absent clavicle, fused carpal elements, a deep acetabulum, and a modified pelvic girdle, constitutes a coherent adaptive suite for a life suspended beneath branches. These features collectively enhance skeletal stability, provide extensive surfaces for the attachment of powerful flexor musculature, and maximize mechanical advantage during climbing and stationary hanging. The absence of a clavicle increases the range of motion in the shoulder, while the pelvic morphology aids in securing the body. Primary limitations of this study include the modest sample size (n=9) and the exclusive use of juvenile specimens, which may affect the generalizability of findings related to ossification completeness (e.g., the unossified patella) and fully mature osteological proportions. The use of cadavers, while standard for anatomical studies, precludes dynamic functional assessment. In conclusions this computed tomography-based anatomical study successfully elucidates the detailed osteology of the *B. variegatus* appendicular skeleton, establishing a clear structure-function relationship for its arboreal and suspensory habits. The findings provide a crucial anatomical benchmark for future comparative, clinical, and evolutionary biology studies, highlighting the sloth as a remarkable model of morphological adaptation to a specialized ecological niche. Further research with adult specimens is warranted to confirm ontogenetic patterns.

Keywords: common sloth, tomography anatomy, suspensory locomotion, musculoskeletal adaptation, xenarthran morphology.

DOI: 10.22456/1679-9216.150901

Received: 12 November 2025 Accepted: 15 February 2025 Published: 5 March 2026

[1]Instituto de Medicina Veterinária (IMV), Universidade Federal do Pará (UFPA), Castanhal, PA, Brazil. [2]Centro de Educação Profissional DNA, Ananindeua, PA. [3]Instituto de Saúde e Produção Animal (ISPA), Universidade Federal Rural da Amazônia (UFRA), Belém, PA. [4]Campus Araguatins, Instituto Federal de Educação, Ciência e Tecnologia do Tocantins (IFTO), Araguatins, TO, Brazil. CORRESPONDENCE: F.D.O. Monteiro [deciomonteiro@ifto.edu.br]. IFTO - Campus Araguatins. Povoado Santa Teresa km 5. CEP 77.950-000 Araguatins, TO, Brazil.

INTRODUCTION

The arboreal lifestyle of the brown-throated sloth (*Bradypus variegatus* Schinz, 1825) differs from other quadrupedal mammals [25,30]. Principles as thorax between the forelimbs, body propulsion through rotation of the limbs on a proximal pivot, and the contribution of trunk movements related to the mammalian quadrupedal locomotor apparatus such as *Tamadua tetradactyla*, *Euphractus sexcinctus* or *Cebus apella* also apply to modern sloths [1,3-5]. The suspensive posture and locomotion of the sloth in arboreal habitat follow the consequences of a body in reverse gravity [6,7]. Anatomical particularities such as hook nails with joint mobility and short scapula and a rounded thorax ease suspensory locomotion [8,9,19].

Anatomical investigations may help to understand the morphological adaptations associated with a given lifestyle of the sloth [10]. Diagnostic imaging methods as CT can provide anatomic details in 3-dimensional [11,12]. CT allows morphological investigation in live animals of the organs and cavities that are difficult to access [13-15, 20]. Research was been morphological description of the skeletal system of several species to help understand what morphological adaptations are associated with a certain lifestyle [4,14,16,45,46]. The morphology of the appendicular skeleton of *B. variegatus* needs to be better elucidated by CT with the aim of relating it to their locomotor adaptations [17-19, 25].

An alternative to understanding the morphological aspects of the appendicular skeleton of the brown-throated sloth is using CT already used to investigates soft tissues, organs, and cavities [2,12]. The objective this study was elucidate the morphological adaptations of the appendicular skeleton in *B. variegatus* using CT (CT), with a focus on understanding the bone structures that facilitate arboreal locomotion and suspensory behavior in the Amazon region, such the limbs, joint configurations and vestigial elements reflecting evolutionary adaptations to an arboreal lifestyle.

MATERIALS AND METHODS

Sample from the study (experimentation with cadavers)

In the present study, 9 frozen corpses of *Bradypus variegatus* were used (6 young males and 3 young females). These samples were frozen at -2°C to -10°C and came from hospital care at the Veterinary Hospital of the Federal University of Pará (UFPA). They were sick animals, native to the Amazon region, close to the municipality of Castanhal, state of Pará, living wild and different populations, which were sent by an environmental agency of the Brazilian state, such as IBAMA (Instituto Brasileiro do Meio Ambiente). These animals were classified as infants when they did not have a characteristic coat dimorphism and were less than 1.2 kg (<1.2 kg), and juvenile or young, when they presented a sexual dimorphism that was greater than 1.2 kg and less than 2.3 kg (1.2 kg - 2.3 kg) [8].

Computed tomography

The cadavers were initially defrosted in running water for approximately 2 h. Then, they were placed in the dorsal decubitus on a rectangular foam pad, with extended forelimbs and extended hind pelvic limbs.

Images were obtained in the craniocaudal direction on a 16-channel helical tomographic device, Model Syngo CT 2009E[1]. The acquisition protocol was 110 kVp, 130 mA, scan time 62.66 s, and delay 3 s, with a field of view (FoV) of 115 x 115 mm.

The thickness of the slices was 5 mm sagittal with 1 mm multiplanar reconstruction (MPR) in the sagittal and dorsal planes. The acquired blocks of cuts were forwarded to the computer-aided design (CAD) software for 3-dimensional reconstruction in VR (volume rendering).

Evaluation of bone structure

After acquiring the images, descriptions and measurements of the longitudinal and transverse anatomic characteristics of the thoracic and pelvic limbs of each specimen were made, using software tools. The adopted nomenclature was based on the Nomina Anatomica Veterinaria (NAV) [22].

Measurements of bone length were made from longitudinal measurements between 2 points, tak-ing into account the proximal and distal limits.

Regarding transverse measurements, they were obtained with the aim of identifying the mediola-teral or craniocaudal diameter of the proximal and distal extremities and of the mid-diaphysis (Figure 1). The pelvic measurements were performed according to the methodology adapted described by Eneroth *et al*. [11], measuring the horizontal distance between: the distance between the transverse diameter of the 2 tubera coxae, the inner distance between the 2 acetabulum,

the distance between the 2 lateral tubera ischiadica, the distance between the 2 medial tubera ischiadica. The diagonal diameter on the right, the diagonal diameter on the left, the sacropubic diameter and the horizontal distance from the ischial spines in the dorsal region were included.

In the ventral region of the pelvis, the horizontal distance between the anterosuperior crista iliaca was measured; horizontal distance between the corpus ossis ilii in its distal 3rd; horizontal distance between the tuberculum pubicum ventrale in the pubic symphysis and the horizontal distance between the tuber ischiadicum (Figure 2A), while in the dorsal region, the horizontal distance of the spina ischiadica was also measured (Figure 2B).

Morphometric analysis was not the subject of the study, although some measurements were taken for morphological description. Furthermore, there was great variation in the size of the animals, which compromises the reliability of the measurements. Data were obtained based on the morphological descriptions of the collected samples, obtaining qualitative data.

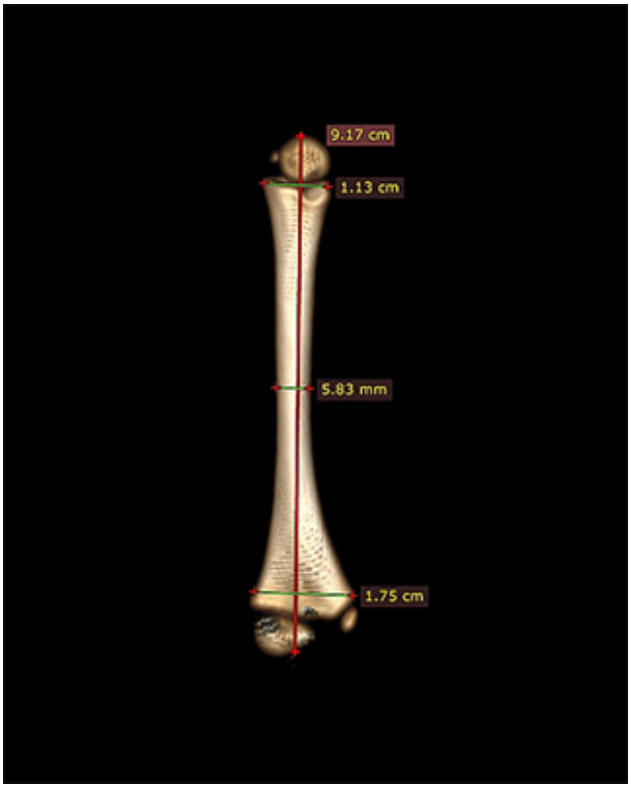


Figure 1. Tomographic image of *Bradypus variegatus* humerus with cranial view. Method of gauging bone structures of the species. Note the longitudinal measurement from the caput humeri (most proximal point of the bone) to the epicondylus medialis (most distal point of the bone). The diameters of the proximal and distal metaphyses, as well as the diaphyseal bone isthmus, were also measured.

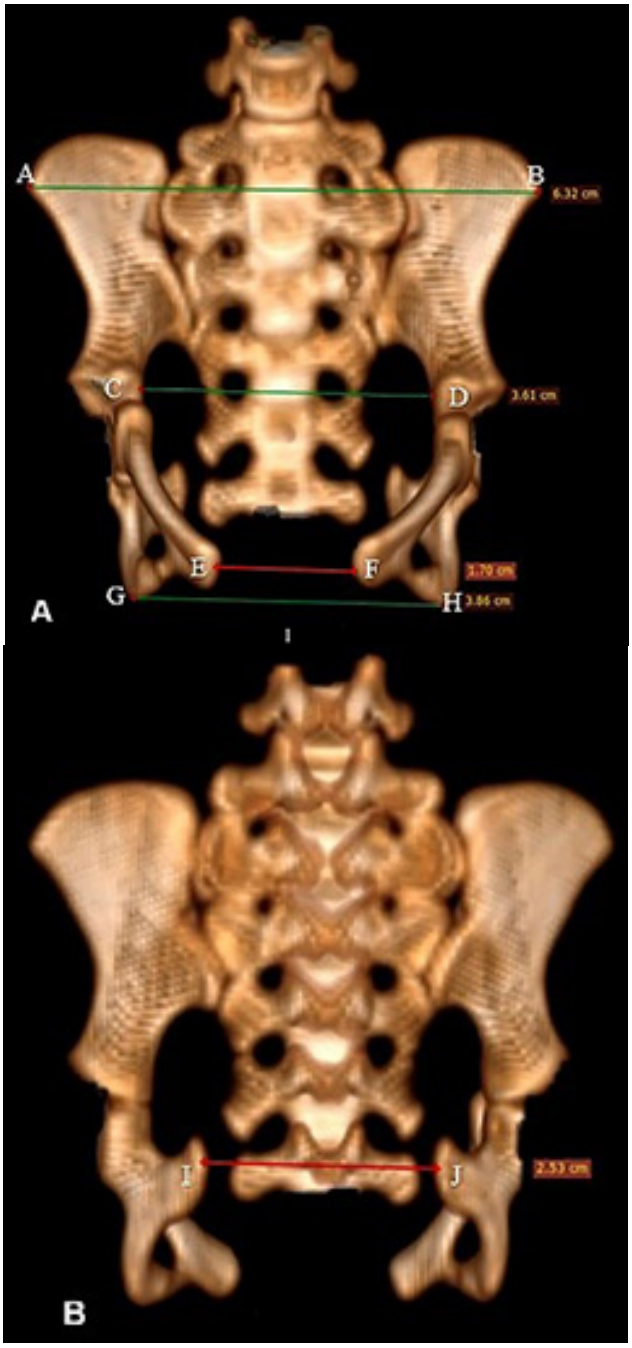


Figure 2. Tomographic image of the pelvis of *Bradypus variegatus* in ventral view (A) and dorsal view (B). Note pelvimetry through horizontal measurements in the ventral region that were performed between the crista iliaca (green line between the points AB), between the caudal portion of the corpus ossis ilii (green line between the points CD), between the pubicum pubicum dorsale (red line between the EF points) and between the tuber ischii (green line between the points GH). The dorsal region was performed between the spina ischiadica (red line between the IJ points).

RESULTS

Forelimb

The scapula was described as a flat bone, proximal to the trunk, and the caudal, cranial, and dorsal margins. The dorsal margin of the scapula is

convex and the ventral margin presents a concavity that strays away from the midline. Regarding the cranial and caudal angle, they were rounded (Figure 3A). The incisura scapulae and the coracoideus process are located cranioventral (Figure 3B).

In terms of scapulae, the cavitas glenoidalis was observed cranially, which has a joint surface fac-ing the ventral margin (Figure 3C). Dorsally there was a bone prominence that projected from the mid-diaphysis, laterocranially, to the cavitas glenoidalis, called the spina scapulae, which divides the supraspinata fossa and the fossa infraspinata, the infra being more elongated than the supra (Figure 3A). On the medial surface, the shallow subscapular fossa enlarged the rib cage. In the cranial part, the presence of the acromion-clavicular joint was not observed (Figure 3D).

The humerus was characterized as a long cylindrical bone with a distance between the proximal and distal ends of 9.17 cm. The diameter of the diaphyseal isthmus was 5.83 mm, the proximal metaphysis was 1.13 cm, and the distal was 1.75 cm (Figure 4A). On the cranial surface of the proximal epiphysis is the caput humeri, which presents a slightly rounded ventral region, articulating with the cavitas glenoidalis of the scapulae, as well as the lesser and greater tubercles (scapulohumeral joint). The distal epiphysis in the craniocaudal direction is flat and the lateral and medial epicondylus was able to visualise. Two structures were also visualised: 1 medial and the other lateral, suggesting the trochlea and capitulum humeri (Figure 4B). A depression was observed at the edge of the proximal epiphysis at the height of the collum humeri in the dorsal region of the humerus. In the distal epiphysis, there is a bone depression located in the medial region of the humerus, suggesting that it is the fossa olecrani and the absence of the supratrochleare foramen (Figure 4A).

The thoracic limbs are composed of the radius and ulna, which present a curvature and an inter-osseous space that completely separates them. The radius is a long and slightly curved bone. In the proximal region, it articulates with the humerus (epycondilus medialis and articulatio cubiti) and distally with the carpus (articulatio radioulnaris).

The radius length was 7.07 cm. The diameter of the mid-diaphysis was 4.63 mm and the mediolateral width of the proximal and distal epiphyses was 7.41 mm and 1.11 cm, respectively (Figure 5A).

In the proximal epiphysis, it was possible to see caput radii with a rounded appearance and its flat joint edge. In the proximal diaphysis, a medial curvature was visualised, which formed a small bony prominence called the tuberositas radii. Distally, near the carpi articulatio in the medial region, the styloideus process was observed (Figure 5B).

The ulna is located laterally in the forearm and attaches to the radius and humerus at its proximal extremity and to the radius at its distal extremity. This bone had a length of 8.19 cm between the epiphyses (from the styloid process of the olecranon to the ulnar axis) and a diameter of the mediolateral diaphysis of 4.17 mm. In its proximal and distal epiphyses, it had a mediolateral diameter of 5.79 and 8.58 mm, respectively (Figure 5A). Cranially, in the proximal epiphysis, a discreet bony protuberance was observed, followed by a slight shallow notch. In the proximal diaphysis, on its medial face, the presence of a groove was identified along the bone surface. The distal epiphysis was found to be substantially displaced from the ulnar metaphysis. The cartilaginous distal ulnar epiphysis is surprisingly long (Figure 5B).

However, in the caudal region, the described structures were observed with the absence of the sulcus on the proximal surface.

Five ossa carpi were identified, diffusely arranged, sliding freely between their joint surfaces, with the 5th carpal bone with the largest dimension fused directly to the base of the metacarpals (Figure 6A).

The presence of bone metacarpalia was observed with the absence of space in the articulatio met-acarpophalangeae and with a 1st carpal bone with a reduction in dimension fused directly to the base of the metacarpals (Figure 6B). The phalanges comprise a total of 9 structures, differing in the follow-ing: proximal, middle, and distal, with the middle being relatively larger. The presence of long claws directly connected to the distal phalanges is highlighted (Figure 6C).

Pelvic limb

The femur presents the diaphysis with a slight curve in the medial direction. The proximal epiphyses, as well as the distal ones, present discontinuity between the connection with the diaphysis, which is the area of the metaphysis. The diaphysis is compact with a mediolateral diameter of 7.51 mm, with a distance

between its epiphyses of 5.87 cm and a width in the proximal and distal thirds of 1.21 cm and 1.60 cm, respectively (Figure 7A).

On the cranial surface of the proximal epiphysis, the caput of the femoris is circular in shape with a flat surface. Laterally, the epiphysis of the trochanter major is observed lateral to the femoris caput, and the trochanter minor is present on the medial side below the femoris caput. In the distal femoral epiphysis, the medial and lateral femoral condyles and respective epicondyles were observed there, and between them, caudally, the intercondylaris fossa. In the femorotibial articulatio, no patella was observed (Figure 7B).

The tibia and fibula are bones that make up the pelvic limb (Figure 8B). The tibia presents at its extremity's articulations with the fibula, which constitutes the articulatio tibiofibularis proximalis and distalis, in addition to a line of metaphysis. It also had a total length of 5.48 cm. The diameter of the diaphyseal isthmus was 4.69 mm. The mediolateral width of the cranial and distal metaphysis was 11.5 and 9.48 mm, respectively (Figure 8A).

It was possible to identify in the tibia, in its proximal cranial portion, the presence of a rough and irregular appearance and a homogeneous distribution on the side in contact with the metaphysis. More distally, it has a triangular shape, showing the tuberositas tibiae (Figure 8A), which corresponds to an area centred on the cranial surface and with a small protrusion that projects in the opposite direction to its central axis. The condylus medialis and the condylus lateralis also stand out as prominent structures that oppose each other (Figure 8B).

Distally from the tibia, the malleolus medialis was observed to be a structure without extensions that differentiate it from the area that opposes it. We could also observe the existence of a flat bone structure with irregular edges and a homogeneous distribution on the face that is in contact with the metaphysis area.

The fibula had a length of 4.90 cm. The thickness of the mid-diaphysis was 3.58 mm, the proximal epiphysis was 4.13 cm and the distal 6.22 cm (Figure 8A). A rounded head with a smooth surface was identified in the proximal epiphysis. In the distal epiphysis, it was possible to observe the malleolus lateralis as a structure without extensions that differentiates it from the area that opposes it (Figure 8B). An oval bone structure with irregular edges and homogeneous distribution was observed on the face that is in contact with the metaphysis area.

Extremities of the pelvic limb

The set of ossa tarsi consists of a total of 5 bones with discrete joint spaces. In relation to the talus, it is the most proximal bone among them; it projects from the median to the medial plane and articulates laterally with the fibula and medially with the tibia, presenting a smooth surface in the cranial direction. Distally, it articulates with the calcaneus navicular (Figure 9A).

The calcaneus is a laterally located bone of irregular dimensions laterally located with a prominent projection facing the caudal portion. It is possible to identify the articulation with the talus, which generates the articulatio talocalcanea, in addition to a concavity facing its ventral surface (Fig-ure 9B).

Navicular is a medial bone without codominance between its linear dimensions. It articulates caudally to the talus, forming the talocalcaneonavicular (TCN), and on its distal surface it communicates with one of the metatarsal bones, forming the tarsal-metatarsal joint.

A set of 3 fused cuneiform bones, located medially, was visualised, formed by fusion of bone pieces with a rough appearance that articulate to the metatarsals (Figure 9B).

The cuboideum is a laterally located bone identified cranial to the calcaneus and distal to the metatarsal.

The presence of ossa metatarsalia I-V was observed, with the 1st and 5th having proportionately smaller dimensions compared to the others. In the 1st metatarsal, it was possible to observe a structure with a conical aspect and a medial location. In the 5th metatarsal, a bone structure with an insinuation facing the lateral portion was identified, articulating with the cuboideum and the metatarsal (Figure 9B).

The phalanges constitute a total of 9 bones arranged, respectively, in the proximal phalanx, the media phalanx, and the phalanx distalis, with the 2nd being relatively larger. Furthermore, the presence of elongated claws directly connected to the distal phalanges was also identified (Figure 9B).

Pelvis

The pelvis is a set of flat and irregular bones of equivalent length and width, with predominance over thickness. The pelvis is made up of a bony triad comprising the ilium, ischium, and pubis (Figure 10A). The ilium articulates with the sacrum to form the articulatio sacroiliaca.

The sacrum refers in its shape to an inverted pyramid with processes spinosus reduced in the caudal direction. This structure has 6 flat vertebral bodies that articulate only the 2nd, 3rd, and 4th vertebrae with the ileum. The sacrum articulates cranially with the 5th lumbar vertebra and at the other end with the caudal vertebrae. These vertebrae present laterally the transverse processes and laterally the spinous process, both poorly developed and reduced in the caudal direction (Figure 10B).

The acetabulum is formed by the union of the ischium, ilium, and pubis, with no connection between the latter two. The acetabulum has a curved and discontinuous shape with a smooth inner surface. The acetabulum region is interrupted in the ventral direction, causing the acetabuli of the fossa. This structure communicates with the foramen obturatum, which in this animal was characterized by a large oval-shaped orifice (Figure 11).

The ilium is a flat and irregularly shaped bone, divided into 2 parts: corpus ossis ilii and ala ossis ilii, separated by the linea arcuata. The distance between the right and left crista iliaca was 6.32 cm and 3.61 cm between their bodies in the distal 3rd (Figure 2A). We did not cheque the ventralis cranial spina iliaca (Figure 2B).

The ischium showed a distance between the right and left tuber ischiadicum of 3.86 cm (Figure 2A). The cranial part of the body of the ischium fuses with the pubis and ilium. The ischii of the ramus ossis connect to the ventral ramus of the pubis to form the ischiopubic ramus, which was thin, constituting the ventral limit of the foramen obturatum, which had an ellipsoid shape (Figure 12). At the dorsal margin of the ischium there is a pointed prominence facing cranially, called the spina ischiadica, which presented a dorsal distance of 2.53 cm (Figure 2B). This structure separates the greater from the incisura ischiadica minor, in which the form can be evidenced by its circular shape, more accentuated compared to the incisura ischiadica minor (Figure 12).

The pubis, being the smallest bone that forms the surface of the symphysialis of the pelvis, presents the right and left facies at the end of the pubic tuberculum, with 1.70 cm (Figure 2A).

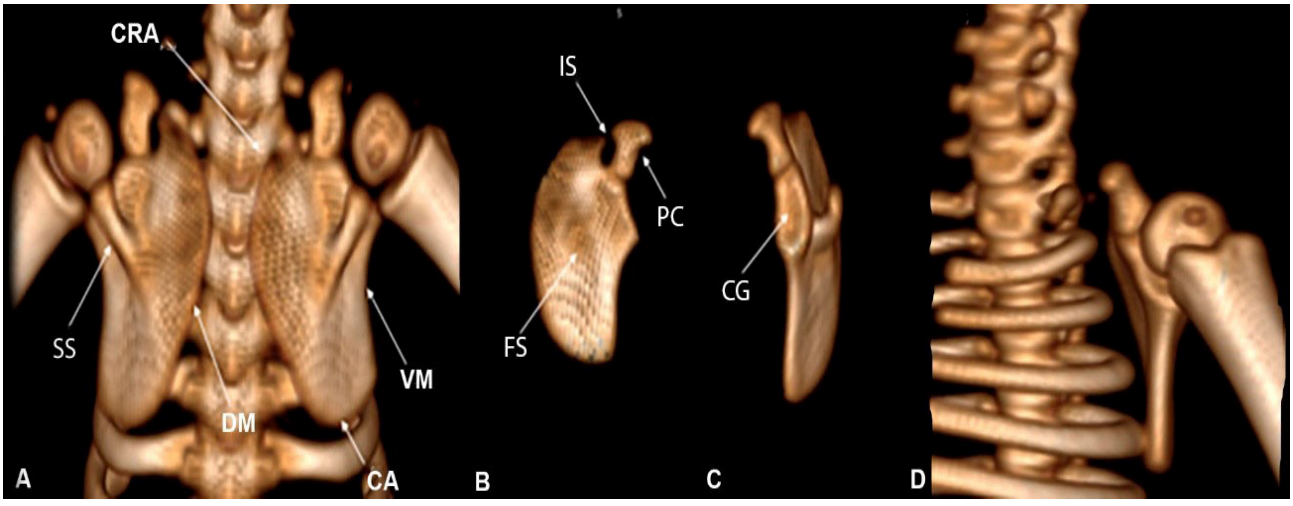


Figure 3. Computed tomography image in *Bradypus variegatus*. A- Dorsal view of the scapula showing the following anatomical structures: cranial angle (CRA), caudal angle (CA), spina scapulae (SS), dorsal margin (DM), ventral margin (VM). B- Midcaudal view showing Incisura scapulae (IS), fossa supraspinata (FS), and process coracoideus (PC). C- Cranial view, cavitas glenoidalis (CG). D- Ventral view showing the absence of the acromion-clavicular joint.

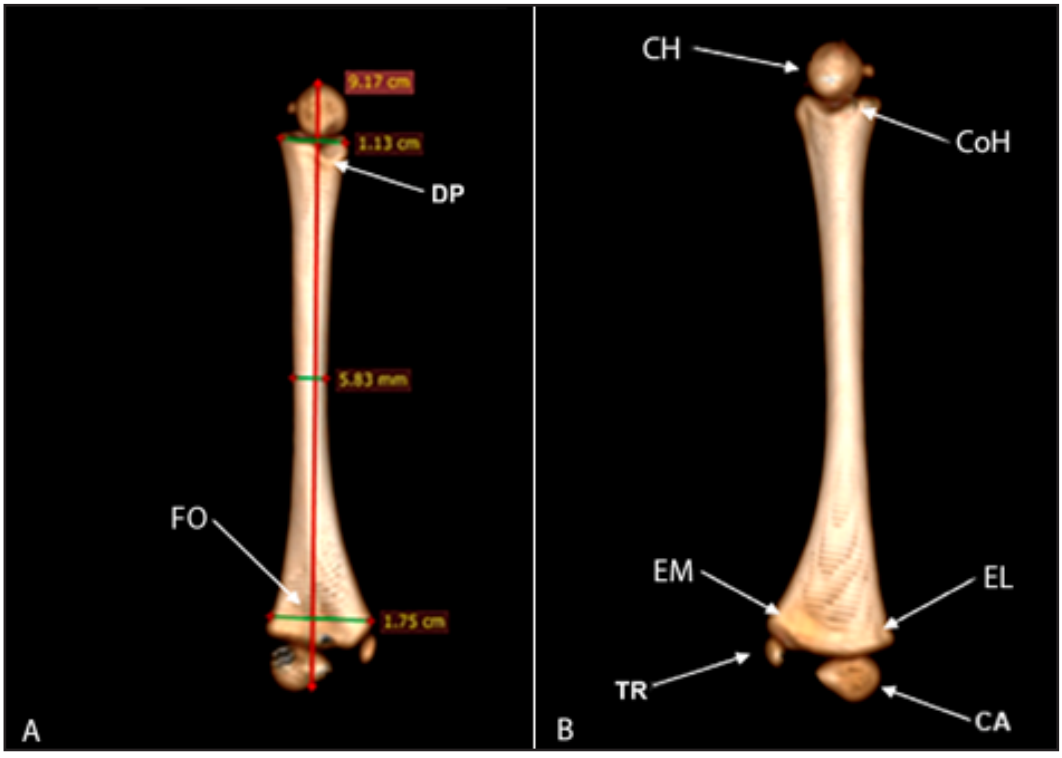


Figure 4. Computed tomography image of the humerus: caudal view of the humerus. A- Measurements of the humerus, depression (DP), and fossa olecrani (FO). B- Cranial view of humerus B, caput humeri (CH), collum humeri (CoH), medial epidondylus (EM), epicondylus lateralis (EL), trochlea (TR), capitulum (CA).

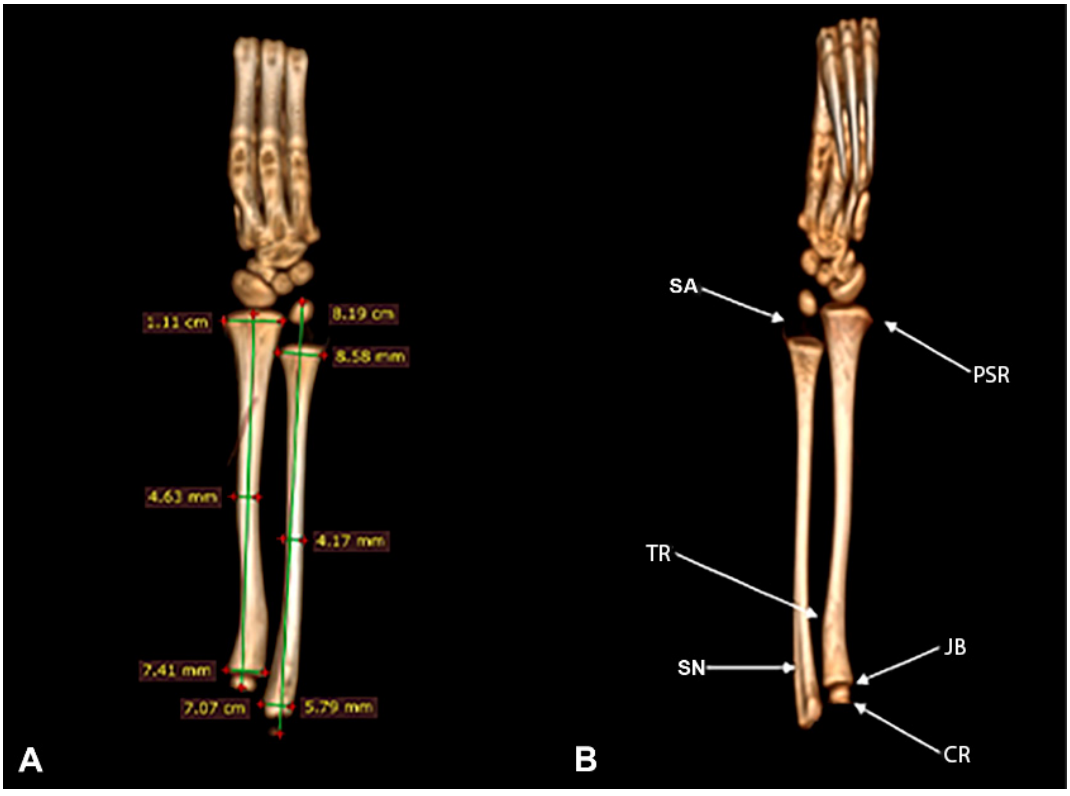


Figure 5. Computed tomography image of radius and ulna of *Bradypus variegatus*. A- Dorsal view, measurements of the radius and ulna. B- Palmar view, caput radii (CR), joint border (JB), tuberositas radii (TR), processus styloideus radii (PSR), shallow notch (SN), spacing area (SA).

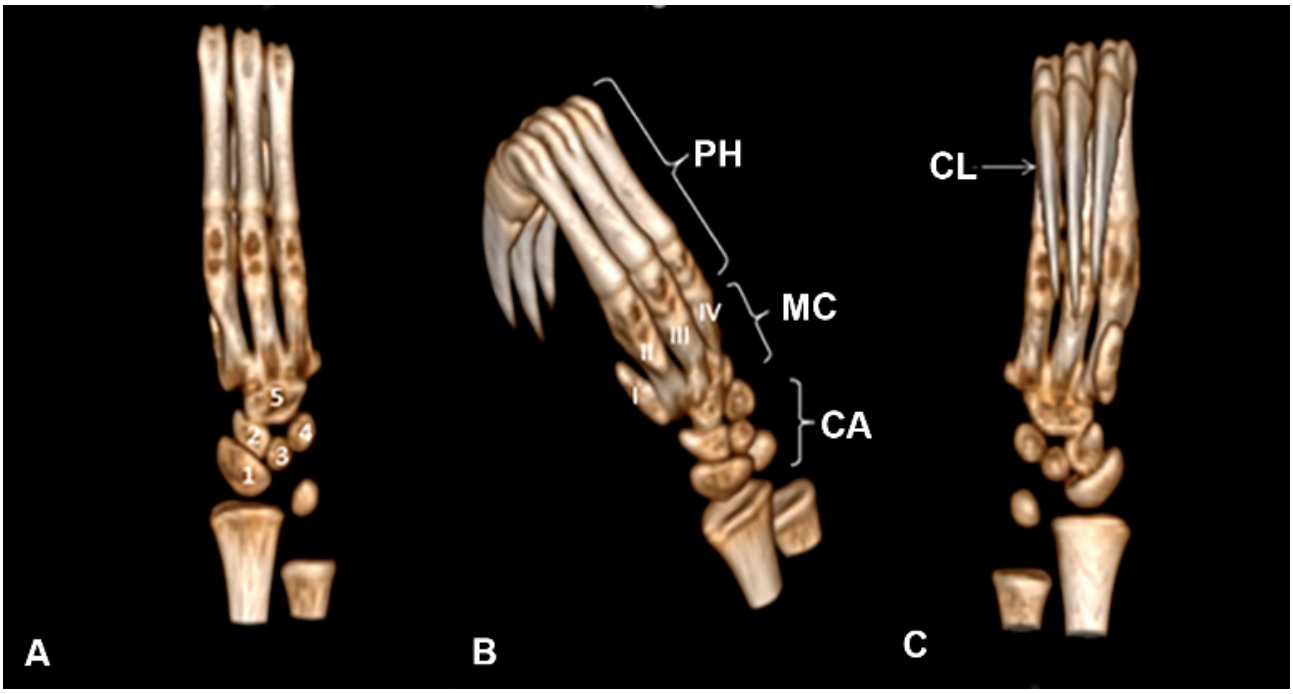


Figure 6. Computed tomography image in *Bradypus variegatus*. A- Dorsal view with the bones of the carpus numbered 1, 2, 3, 4, and 5. B- Oblique view, oss carpi (CA), ossa metacarpalia (MC) I-V, and phalanges (PH). C- Ventral view (palmar), claw (CL).

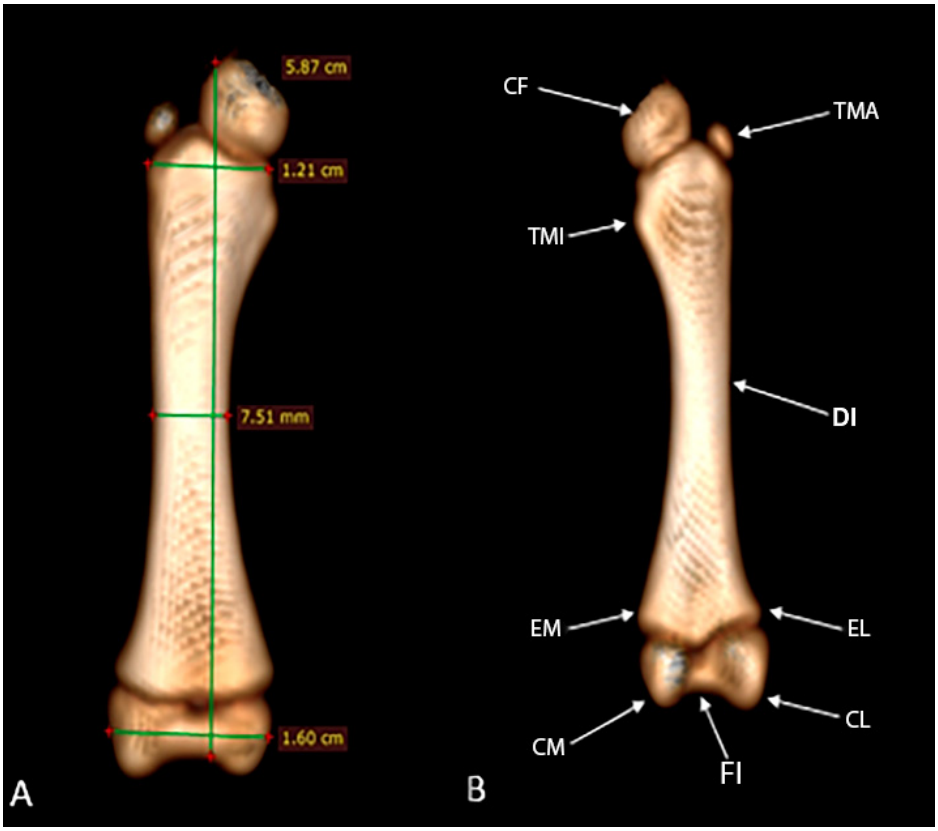


Figure 7. Computed tomography image of the femur of *Bradypus variegatus*. A- Dorsal view, femur measurements. B- Caudal view, caput ossis femoris (CF), trochanter major (TMA), trochanter minor (TMI), diaphysis (DI), epicondylus lateralis (EL), epicondylus medialis (EM), condylus lateralis (CL), condylus medialis (CM), fossa intercondylaris (FI).

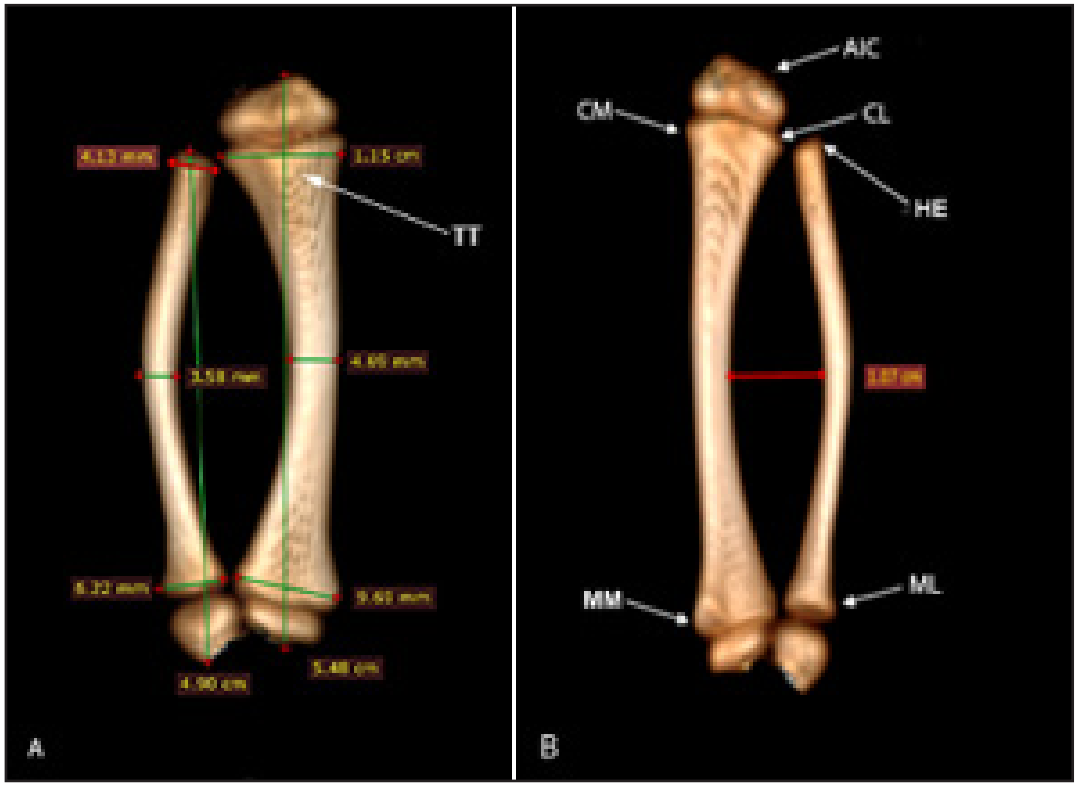


Figure 8. Computed tomography image in *Bradypus variegatus*. A- Dorsal view, tuberositas tibiae (TT), tibia and fibula measurements. B- Dorsal view, intercondylaris cranialis (AIC), condylus lat-eralis (CL), condylus medialis (CM), head (HE), malleolus lateralis (ML), malleolus medialis (MM).

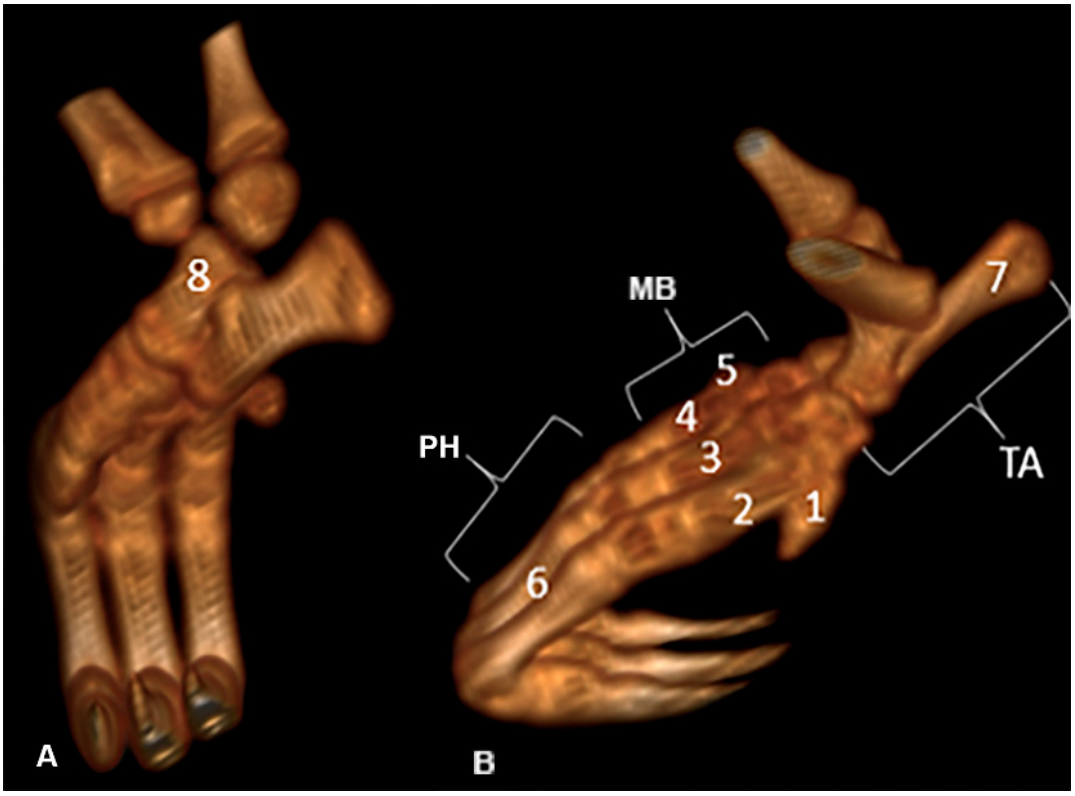


Figure 9. Computed tomography image of the distal extremity of the pelvic member of *Bradypus variegatus*. A- Plantar oblique view, showing the talus (8). B- dorsal oblique view, tarsus (TA), calca-neus (7), numbers 1,2,3,4,5 correspond to ossa metatarsalia I-V (MB), and 6, to the phalanges (PH).

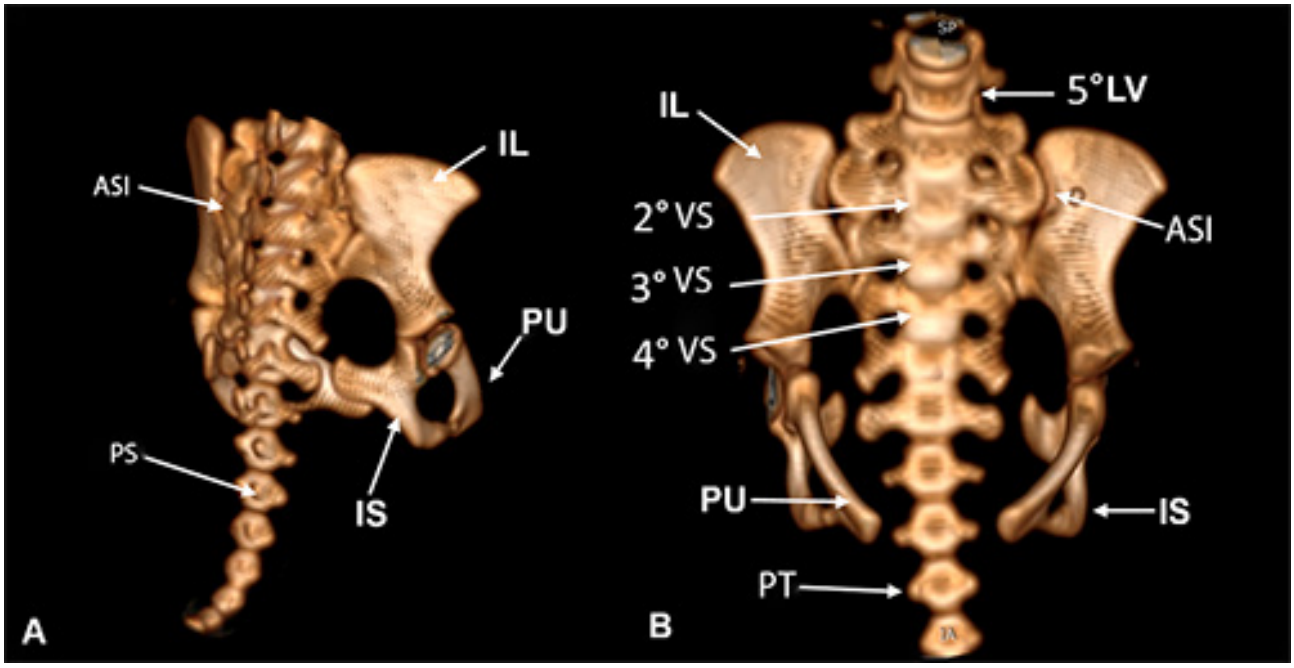


Figure 10. Pelvis in *Bradypus variegatus*. A- Dorsal view, articulatio sacroiliaca (ASI), process spi-nosus (PS), ileum (IL), pubis (PU), ischium (IS). B- Cranial view, ileum (IL), sacrales vertebrae (VS), pubis (PU), transversus (PT), lumbar vertebra (LV), articulatio sacroiliaca (ASI), ischium (IS).

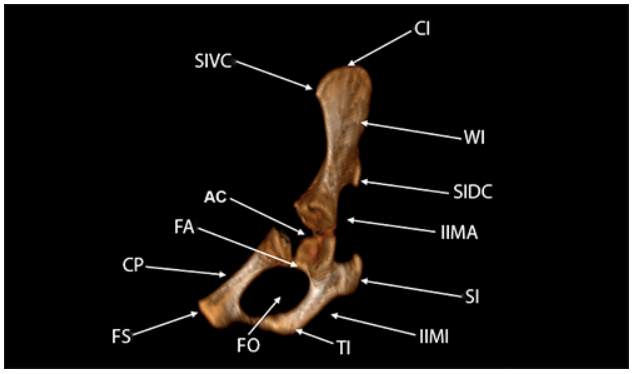


Figure 11. Computed tomography image of the pelvini ossa member of the common sloth (*Bradypus variegatus*). Left side view. Spina iliaca ventralis caudalis (SIVC), acetabulum (AC), fossa acetabuli (FA), corpus ossis pubis (CP), facies symphysialis (FS), foramen obturatum (FO), tuber ischiadicum (TI), incisura ischiadica minor (IIMI), spina ischiadica (SI), incisura ischiadica major (IIMA), spina iliaca dorsalis caudalis (SIDC), ala ossis ilii (WI), crista iliaca (CI).

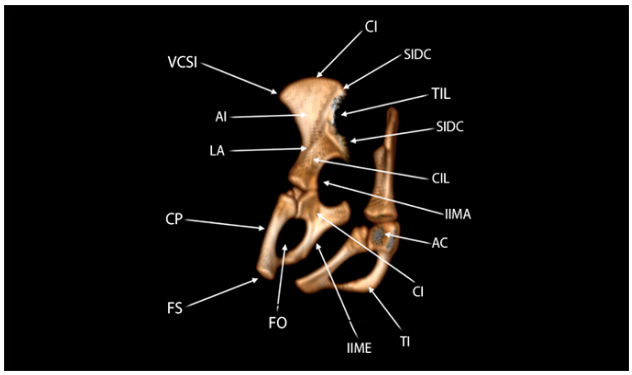


Figure 12. Computed tomography image of the pelvis of the common sloth (*Bradypus variegatus*). Side view, ventral-cranial spina iliaca (VCSI), ala ossis ilii (AI), linea arcuata (LA), corpus ossis pubis (CP), facies symphysialis (FS), foramen obturatum (FO), incisura ischiadica minor (IIME), tuber is-chiadicum (TI), corpus ossis ischii (CI), acetabulum (AC), incisura ischiadica major (IIMA), corpus ossis ilii (CIL), spina iliaca dorsalis caudalis (SIDC), tuberositas iliaca (TIL), spina iliaca dorsalis cra-nialis (SIDC), crista ilaca (CI).

DISCUSSION

The appendicular skeleton of *B. variegatus* is similar to *Choloepus didactylus* [18,47]. Furthermore, the larger pectoral limbs compared to the pelvic limbs, including the oblique scapular spine and more pronounced muscular development in these limbs with a small range of abduction are morphological aspects found in this species. The shape of bone morphological conformations, such as protuberances, concavities, or discontinuities in bone tissue, may be associated with movement and locomotion with a small range of limb abduction in these species [24,27,28].

The larger thoracic limbs compared to the pelvic limbs are a morphology of the bones that

shows a characteristic of the species. It is a peculiar aspect of *Bradypus*, but having forelimbs (or thoracic limbs) longer than the hindlimbs (or pelvic limbs) is not a unique characteristic of this species. Mammals that perform suspensions and/or climbs generally have this characteristic (e.g., orangutans, gorillas) [29,33,40,41].

Phylogenetic and molecular data showed that *Bradypus* and *Choloepus* evolved independently, that is, they are not a monophyletic group. However, they are very similar in behaviour and morphology, with an arboreal lifestyle and characteristic locomotion, the result of shared ancestry [10,12,32,34]. Thus, the musculoskeletal structure was adapted to perform suspensory posture and movements and to accommodate the reduced body muscle mass resulting from its diet based on leaves, sprouts, and fruits [15,21,32].

There are discrepancies with respect to the existence of a clavicle in *B. variegatus*. The presence of this bone is described in some studies and not in others. The clavicle has been described in young sloths and has disappeared or being rudimentary in adults. The clavicle was not observed in this study. This allows us to advise that this structure cannot be used as a reference for the identification of this species, as there is individual variation; however, we reinforce the need for more extensive investigations to identify it in a larger population of individuals [21,23,34,35].

In studies carried out by Miller [26], Hautier *et al*. [21] and Nyakatura & Fischer [34] this variation in relation to the presence of the clavicle was reported. Miller [26] cites the clavobrachialis muscle of this species to strengthen the insertion of the deltoid and vestigial clavicle. When describing the forelimbs in sloths he reports that 1 and 5 metacarpals are vestigial, in *Choloepus* 1 and 4 metacarpals are vestigial. In view of what has been observed, we can consider this structure as a vestigial organ. In summary, the relationship between the sloth and the clavicle as a vestigial organ is related to the arboreal habits of these animals and their characteristic locomotion. The presence or absence of the clavicle can vary between individuals, but its functional importance has been reduced due to adaptation to their natural environment [5,17-19].

The inconsistent pattern of ossification in *B. variegatus* justifies incomplete bone fusion of some structures [20]. In the radius and ulna, interosseous spaces similar to those seen in humans were found, with spacing in the distal epiphysis of the ulna. Some structures may or may not be fused; however, the inconsistency of ossification in this species allows us to hypothesize a divergent line from the common being [13,22,41]. Bones that do not fully fuse in adults are also quite common in marsupials, reflecting growth rates and life history strategies [43,44].

In the carpal region, 5 fused bones were identified, different from other species such as giant anteaters and nonhuman primates. Fusion of these bones restricts wrist movements, and claws work as "pincers" adapted to hang and move in natural habitat, hypertrophying the flexor musculature in the finger along the forearm [36,37,39]. Therefore, we believe that since these animals spend most of their time hanging, they adapted and consequently there was a disproportion in these structures, since the pelvic limbs are used as a support point that functions as a "hook" in the tree trunks to increase the moment of displacement, facilitating the suspensory effect of the forelimbs [33,38,42].

The pelvic limbs are smaller than the pectoral limbs, indicating that they play a less important role in sloth locomotion than in typical arboreal quadrupeds. Therefore, the pelvic limb has a lower proportion than the humerus and the absence of a patella, which does not have a preponderant morphophysiological function in this species. The absence of patella could be due to the lack of ossification in this juvenile specimen. The lack of a patella in an adult is needed to confirm this observation. The tibia and fibula presented an irregular interosseous space that is articulated with the intercondylar notch, a finding similar to those found by Montilla-Rodríguez *et al*. [29] who described the triangular-shaped structure in the proximal epiphysis of the tibia.

The spinal and transverse processes of the caudal vertebrae can present changes in shape and development in *B. variegatus*, even in the same animal, depending on adaptation and behaviour [47,48]. The pelvis in Xernathra is similar, the ischial spine is turned cranially, with a thin ischial tuberosity, and the pubis with lateral amplitude, probably due to the fact that the sloth moves and attaches itself to the tree trunks. The rounded and deep acetabulum and the absence of the ventrocaudal iliac spine ensure the stability of the animal's body [16,31,32].

CONCLUSIONS

Based on these results, it was possible to describe in detail the bone structures of the limbs and pelvis of *Bradypus variegatus*, demonstrating the pronounced development of thoracic limbs compared to pelvic limbs, the absence of a clavicle (suggesting vestigially), and structural adaptations such as a rounded acetabulum and laterally wide pubis, fused carpal bones and elongated claws, which enhance stability and muscle attachment for arboreal mobility and life. These features align with the sloth's unique suspensory lifestyle and reflect evolutionary adaptations to its environment, contributing to broader discussions in evolutionary biology, biomechanics, and conservation. Limitations such as sample size and the absence of adult specimens warrant further investigation to deepen our understanding of these adaptations.

MANUFACTURER

[1]Siemens. Forchheim, Germany.

***Acknowledgements*.** The authors gratefully thank the team of video surgery, obstetrics and reproduction group (VOR), the National Council for Scientific and Technological Development (CNPq, Brazil), the Coordination for the Improvement of Higher Education Personnel (CAPES, Brazil) and the Research and Postgraduate Pro-Rector of Pará Federal University (Propesp/UFPA) for financial support in the study.

***Ethical approval*.** The present study was conducted after the approval of the Animal Ethics and Welfare Committee of the Federal University of Pará (protocol No. 5943220321). The ethics principles of the European Commission for animal experiments involving animals (Directive 86/609EEC) were also followed.

***Declaration of of interest*.** The authors report no conflicts of interest. The authors alone are responsible for the content and writing of the paper.

REFERENCES

1 **Amson E. & Nyakatura J.A. 2018.** The postcranial musculoskeletal system of xenarthrans: insights from over two centuries of research and future directions. *Journal of Mammalian Evolution*. 25: 459-484. DOI: 10.1007/s10914-017-9408-7

2 **Borges N.C., Cruz V.S., Fares N.B., Cardoso J.R. & Bragato N. 2017.** Morphological evaluation of the thoracic, lumbar and sacral column of the giant anteater (*Myrmecophaga tridactyla* Linnaeus, 1758). *Pesquisa Veterinária Brasileira*. 37(4): 401-407. DOI: 10.1590/s0100-736x2017000400016

3 **Borges N.C., Nardotto J.R.B., Oliveira R.S.L., Rüncos L.H.E., Ribeiro R.G. & Bogoevich A.M. 2017.** Anatomy description of cervical region and hyoid apparatus in living giant anteaters *Myrmecophaga tridactyla* Linnaeus, 1758. *Pesquisa Veterinária Brasileira*. 37(11): 1345-1351. DOI: 10.1590/s0100-736x2017001100025

4 **Buckland W. 1834.** On the adaptation of the structure of the sloths to their peculiar mode of Life. *Transactions of the Linnean Society of London*. 17(1): 17-27. DOI: 10.1111/j.1095-8339.1834.tb00015.x

5 **Butcher M.T., Morgan D.M., Spainhower K.B., Thomas D.R., Chadwell B.A., Avey-Arroyo J.A., Kennedy S.P. & Cliffe R.N. 2022.** Myology of the pelvic limb of the brown-throated three-toed sloth (*Bradypus variegatus*). *Journal of Anatomy*. 240(6): 1048-1074. DOI: 10.1111/joa.13626

6 **Cardoso J.R., Souza P.R., Cruz V.S., Benetti E.J., Silva M.S.B., Moreira P.C., Cardoso A.A.L., Martins A.K., Abreu T., Simões K. & Guimarães F.R. 2013.** Anatomical study of the lumbosacral plexus of the *Tamandua tetradactyla*. *Arquivo Brasileiro de Medicina Veterinária e Zootecnia*. 65(6): 1720-1728. DOI: 10.1590/S0102-09352013000600020

7 **Casali D.M., Boscaini A., Gaudin T.J. & Perini F.A. 2022.** Reassessing the phylogeny and divergence times of sloths (Mammalia: Pilosa: Folivora), exploring alternative morphological partitioning and dating models. *Zoological Journal of the Linnean Society*. 196(4): 1505-1551. DOI: 10.1093/zoolinnean/zlac041

8 **Castro-Vásquez L., Meza M., Plese T. & Moreno-Mora S. 2010.** Activity patterns, preference and use of floristic resources by *Bradypus variegatus* in a tropical dry forest fragment, Santa Catalina, Bolívar, Colombia. *Edentata*. 11:62-69. DOI: 10.1896/020.011.0111

9 **Cunha M.S., Albuquerque R.S., Campos J.G.M., Monteiro F.D.O., Rossy K.C., Cardoso T.S., Carvalho L.S., Borges L.P.B., Domingues S.F.S., Thiesen R., Thiesen R.M.C. & Teixeira P.P.M. 2024.** Computed Tomography Evaluation of Frozen or Glycerinated *Bradypus variegatus* Cadavers: A Comprehensive View with Emphasis on Anatomical Aspects. *Animals*. 14(3): 355. DOI: 10.3390/ani14030355

10 **Delsuc F., Kuch M., Gibb G.C., Karpinski E., Hackenberger D., Szpak P., Martínez J.G., Mead J.I., McDonald H.G., MacPhee R.D.E., Billet G., Hautier L. & Poinar H.N. 2019.** Ancient Mitogenomes Reveal the Evolutionary History and Biogeography of Sloths. *Current Biology*. 29(12): 2031-2042. DOI: 10.1016/j.cub.2019.05.043

11 **Eneroth A., Linde-Forsberg C., Uhlhorn M. & Hall M. 1999.** Radiographic pelvimetry for assessment of dystocia in bitches: a clinical study in two terrier breeds. *Journal of Small Animal Practice*. 40(6): 257-264. DOI: 10.1111/j.1748-5827.1999.tb03076.x

12 **Gaudin T.J. 2004.** Phylogenetic relationships among sloths (Mammalia, Xenarthra, Tardigrada): the craniodental evidence. *Zoological Journal of the Linnean Society*. 140(2): 255-305. DOI: 10.1111/j.1096-3642.2003.00100.x

13 **Gavazzi L.M., Kjosness K.M. & Reno P.L. 2021.** Ossification pattern of the unusual pisiform in two-toed (*Choloepus*) and three-toed sloths (*Bradypus*). *Anatomical Record*. 305(7): 1804-1819. DOI: 10.1002/ar.24832

14 **Gebo D.L. 1996.** Climbing, brachiation, and terrestrial quadrupedalism: Historical precursors of hominid bipedalism. *American Journal of Physical Anthropology*. 101(1): 55-92. DOI: 10.1002/(SICI)1096-8644(199609)101:1<55::AID-AJPA5>3.0.CO;2-C

15 **Gilmore D.P., Costa C.P. & Duarte D.P.F. 2001.** Sloth biology: an update on their physiological ecology, behavior and role as vectors of arthropods and arboviruses. *Brazilian Journal of Medical and Biological Research*. 34(1): 9-25. DOI: 10.1590/S0100-879X2001000100002

16 **Gorvet M.A., Wakeling J.M., Morgan D.M., Segura D.H., Avey-Arroyo J. & Butcher M.T. 2020.** Keep calm and hang on: EMG activation in the forelimb musculature of three-toed sloths (*Bradypus variegatus*). *Journal of Experimental Biology*. 223(14): jeb218370. DOI: 10.1242/jeb.218370

17 **Grand T.I. 1978.** Adaptations of tissue and limb to facilitate moving and feeding in arboreal folivores. In: Montgomery G.G. (Ed). *The Ecology of Arboreal Folivores*. Washington D.C.: Smithsonian Institution Press, pp.231-241.

18 **Granatosky M.C., Karantanis N.E., Rychlik L. & Youlatos D. 2017.** A suspensory way of life: Integrating locomotion, postures, limb movements, and forces in two-toed sloths *Choloepus didactylus* (Megalonychidae, Folivora, Pilosa). *Journal of Experimental Zoology Part A: Ecological and Integrative Physiology*. 329(10): 570-588. DOI: 10.1002/jez.2221

19 **Grass A.D. 2019.** Inferring differential behavior between giant ground sloth adults and juveniles through scapula morphology. *Journal of Vertebrate Paleontology*. 39(1): e1569018. DOI: 10.1080/02724634.2019.1569018

20 **Hautier L., Weisbecker V., Goswami A., Knight F., Kardjilov N. & Asher R.J. 2011.** Skeletal ossification and sequence heterochrony in xenarthran evolution. *Evolution & Development*. 13(5): 460-476. DOI: 10.1111/j.1525-142X.2011.00503.x

21 **Hautier L., Weisbecker V., Sánchez-Villagra M.R., Goswami A. & Asher R.J. 2010.** Skeletal development in sloths and the evolution of mammalian vertebral patterning. *Proceedings of the National Academy of Sciences*. 107(44): 18903-18908. DOI: 10.1073/pnas.1010335107

22 **International Committee on Veterinary Gross Anatomical Nomenclature. 2017.** Nomina Anatomica Veterinaria. 6th edn. *Editorial Committee*, Hannover, Ghent, Columbia, Rio de Janeiro. 178p.

23 **Kaup M., Trull S. & Hom E.F.Y. 2021.** On the move: sloths and their epibionts as model mobile ecosystems. *Biological Reviews*. 96(6): 2638-2660. DOI: 10.1111/brv.12773

24 **Li Z. & Clarke J.A. 2016.** The Craniolingual Morphology of Waterfowl (Aves, Anseriformes) and Its Relationship with Feeding Mode Revealed Through Contrast-Enhanced X-Ray Computed Tomography and 2D Morphometrics. *Evolutionary Biology*. 43: 12-25. DOI: 10.1007/s11692-015-9345-4

25 **Mendel F.C. 1985.** Use of hands and feet of three-toed sloths (*Bradypus variegatus*) during climbing and terrestrial locomotion. *Journal of Mammalogy*. 66(2): 359-366.

26 **Miller R.A. 1935.** Functional Adaptations in the Forelimb of the Sloths. *Journal of Mammalogy*. 16(1): 38-51. DOI: 10.2307/1374529

27 **Mohamad J.R.J., González-Rodríguez E., Arencibia A., Déniz S., Carrascosa C. & Encinoso M. 2023.** Anatomical Description of Loggerhead Turtle (*Caretta caretta*) and Green Iguana (*Iguana iguana*) Skull by Three-Dimensional Computed Tomography Reconstruction and Maximum Intensity Projection Images. *Animals*. 13(4): 621. DOI: 10.3390/ani13040621

28 **Montañez-Rivera I., Nyakatura J.A. & Amson E. 2018.** Bone cortical compactness in 'tree sloths' reflects convergent evolution. *Journal of Anatomy*. 233(5): 580-591. DOI: 10.1111/joa.12873

29 **Montilla-Rodriguez M.A., Blanco-Rodriguez J.C., Nastar-Ceballos R.N. & Munoz-Martinez L.J. 2016.** Descripción Anatómica de *Bradypus variegatus* em la Amazonia Colombiana (Estudio Preliminar). *Revista de la Facultad de Ciencias Veterinarias*. 57: 3-14.

30 **Moraes-Barros N.D., Giorgi A.P., Silva S. & Morgante J.S. 2010.** Reevaluation of the Geographical Distribution of *Bradypus tridactylus* Linnaeus, 1758 and *B. variegatus* Schinz, 1825. *Edentata*. 11(1): 53-61. DOI: 10.1896/020.011.0110

31 **Morgan D.M., Spainhower K.B., Mossor A.M., Avey-Arroyo J.A. & Butcher M.T. 2023.** Muscle architectural properties indicate a primary role in support for the pelvic limb of three-toed sloths (*Bradypus variegatus*). *Journal of Anatomy*. 242(4): 741-753. DOI: 10.1111/joa.13884

32 **Mossor A.M., Young J.W. & Butcher M.T. 2022.** Does a suspensory lifestyle result in increased tensile strength? Organ-level material properties of sloth limb bones. *Journal of Experimental Biology*. 225(5): jeb242866. DOI: 10.1242/jeb.242866

33 **Myatt J.P., Crompton R.H., Payne-Davis R.C., Vereecke E.E., Isler K., Savage R., D'Août K., Günther M.M. & Thorpe S.K.S. 2012.** Functional adaptations in the forelimb muscles of non-human great apes. *Journal of Anatomy*. 220(1): 13-28. DOI: 10.1111/j.1469-7580.2011.01443.x

34 **Nyakatura J.A. & Fischer M.S. 2010.** Functional morphology and three-dimensional kinematics of the thoraco-lumbar region of the spine of the two-toed sloth. *Journal of Experimental Biology*. 213: 4278-4290. DOI: 10.1242/jeb.047647

35 **Nyakatura J.A. & Stark H. 2015.** Aberrant back muscle function correlates with the intramuscular architecture of the dorsovertebral muscles in two-toed sloths. *Mammalian Biology*. 80(2): 114-121. DOI: 10.1016/j.mambio.2015.01.002

36 **Olson R.A., Glenn Z.D., Cliffe R.N. & Butcher M.T. 2018.** Architectural Properties of Sloth Forelimb Muscles (Pilosa: Bradypodidae). *Journal of Mammalian Evolution*. 25: 573-588. DOI: 10.1007/s10914-017-9411-z

37 **Pereira F.M.A.M., Bete S.B.S., Inamassu L.R., Mamprim M.J. & Schimming B.C. 2020.** Anatomy of the skull in the capybara (*Hydrochoerus hydrochaeris*) using radiography and 3D computed tomography. *Anatomia, Histologia, Embryologia*. 49(3): 317-324. DOI: 10.1111/ahe.12531

38 **Pérez S., Encinoso M., Corbera J.A., Morales M., Arencibia A., González-Rodríguez E., Déniz S., Melián C., Suárez-Bonnet A. & Jaber J.R. 2021.** Cranial Structure of Varanus komo-doensis as Revealed by Computed-Tomographic Imaging. *Animals*. 11(4): 1078. DOI: 10.3390/ani11041078

39 **Presslee S., Slater G.J., Pujos F., Forasiepi A.M., Fischer R., Molloy K., Mackie M., Olsen J.V., Kramarz A., Taglioretti M., Scaglia F., Lezcano M., Lanata J.L., Southon J., Feranec R., Bloch J., Hajduk A., Martin F.M., Gismondi R.S., Reguero M., de Muizon C., Greenwo-od A., Chait B.T., Penkman K., Collins M. & De MacPhee R. 2019.** Palaeoproteomics resolves sloth relationships. *Nature Ecology & Evolution*. 3: 1121-1130. DOI: 10.1038/s41559-019-0909-z

40 **Püschel T.A. & Sellers W.I. 2016.** Standing on the shoulders of apes: Analyzing the form and function of the hominoid scapula using geometric morphometrics and finite element analysis. *American Journal of Biological Anthropology*. 159(2): 325-341. DOI: 10.1002/ajpa.22882

41 **Ruff C.B., Junno J.-A., Burgess M.L., Canington S.L., Harper C., Mudakikwa A. & McFarlin S.C. 2022.** Body proportions and environmental adaptation in gorillas. *American Journal of Physical Anthropology*. 177(3): 501-529. DOI: 10.1002/ajpa.24443

42 **Spainhower K.B., Metz A.K., Yusuf A.R.S., Johnson L.E., Avey-Arroyo J.A. & Butcher M.T. 2021.** Coming to grips with life upside down: How the type of myosin fibre and metabolic properties of sloth hindlimb muscles contribute to suspensory function. *Journal of Comparative Physiology B*. 191: 207-224. DOI: 10.1007/s00360-020-01325-x

43 **Spear J.K. & Williams S.A. 2020.** Mosaic patterns of homoplasy accompany the parallel evolution of suspensory adaptations in the forelimb of tree sloths (Folivora: Xenarthra). *Zoological Journal of the Linnean Society*. 193(2): 445-463. DOI: 10.1093/zoolinnean/zlaa154

44 **Werning S. 2013.** Osteohistological differences between marsupials and placental mammals reflect both growth rates and life history strategies. *Integrative and Comparative Biology*. 53: E224.

45 **White J.L. 1993.** Indicators of locomotor habits in xenarthrans: Evidence for locomotor heterogeneity among fossil sloths. *Journal of Vertebrate Paleontology*. 13(2): 230-242. DOI: 10.1080/02724634.1993.10011502

46 **Withers P.J., Bouman C., Carmignato S., Cnudde V., Grimaldi D., Hagen C.K., Maire E., Manley M., Du Plessis A. & Stock S.R. 2021.** X-ray computed tomography. *Nature Reviews Methods Primer*s. 1: 18. DOI: 10.1038/s43586-021-00015-4

47 Young M.W., McKamy A.J., Dickinson E., Yarbro J., Ragupathi A., Guru N., Avey-Arroyo J.A., Butcher M.T. & Granatosky M.C. 2023. Three toes and three modes: Dynamics of terrestrial, suspensory, and vertical locomotion in brown-throated three-toed sloths (Bradypodidae, Xe-narthra). *Journal of Experimental Zoology Part A: Ecological and Integrative Physiology*. 339(4): 383-397. DOI: 10.1002/jez.2684

48 Zehtabvar O., Masoudifard M., Rostami A., Akbarein H., Sereshke A.H.A., Khanamoeiashi M. & Borgheie F. 2023. CT anatomy of the lungs, bronchi, and trachea in the mature Guinea pig (*Cavia porcellus*). *Veterinary Medicine and Science*. 9(3): 1179-1193. DOI: 10.1002/vms3.1131